

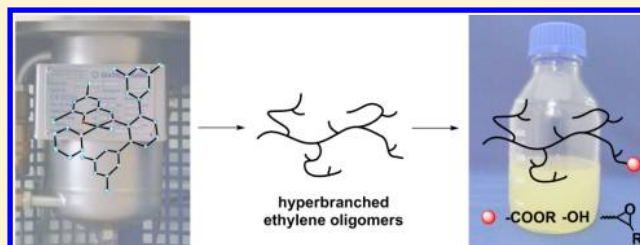
## Monofunctional Hyperbranched Ethylene Oligomers

Thomas Wiedemann, Gregor Voit, Alexandra Tchernook, Philipp Roesle, Inigo Göttker-Schnetmann, and Stefan Mecking\*

Chair of Chemical Materials Science, Department of Chemistry, University of Konstanz, 78464 Konstanz, Germany

**S** Supporting Information

**ABSTRACT:** The neutral  $\kappa^2N,O$ -salicylaldiminato Ni(II) complexes  $[\kappa^2N,O-\{(2,6-(3',5'-R_2C_6H_3)_2C_6H_3-N=C(H)-(3,5-I_2-2-O-C_6H_2)\})NiCH_3(\text{pyridine})]$  (**1a-pyr**, R = Me; **1b-pyr**, R = Et; **1c-pyr**, R = *i*Pr) convert ethylene to hyperbranched low-molecular-weight oligomers ( $M_n$  ca. 1000 g mol<sup>-1</sup>) with high productivities. While all three catalysts are capable of generating hyperbranched structures, branching densities decrease significantly with the nature of the remote substituent along Me > Et > *i*Pr and oligomer molecular weights increase. Consequently, only **1a-pyr** forms hyperbranched structures over a wide range of reaction conditions (ethylene pressure 5–30 atm and 20–70 °C). An in situ catalyst system achieves similar activities and identical highly branched oligomer microstructures, eliminating the bottleneck given by the preparation and isolation of Ni–Me catalyst precursor species. Selective introduction of one primary carboxylic acid ester functional group per highly branched oligoethylene molecule was achieved by isomerizing ethoxycarbonylation and alternatively cross metathesis with ethyl acrylate followed by hydrogenation. The latter approach results in complete functionalization and no essential loss of branched oligomer material and molecular weight, as the reacting double bonds are close to a chain end. Reduction yielded a monoalcohol-functionalized oligomer. Introduction of one reactive epoxide group per branched oligomer occurs completely and selectively under mild conditions. All reaction steps involved in oligomerization and monofunctionalization are efficient and readily scalable.



### INTRODUCTION

Beyond the well-known applications of polyethylenes such as HDPE and LDPE as thermoplastic materials, lower molecular weight ethylene oligomers can serve numerous functions. Concerning their synthesis, the Ziegler Alfol process is an illustrative and practically important example.<sup>1</sup> Chain growth on aluminum yields longer chain aluminum alkyls. Subsequent oxidation and hydrolysis affords linear long-chain terminal alcohols, stoichiometric in aluminum. Chain growth on metallocenes with simultaneous chain transfer reactions is employed for the production of linear polyethylene waxes.<sup>2</sup> These are also functionalized by oxidation under severe conditions, to yield linear oligoethylenes with an undefined number of a mixture of different functional groups (primarily carboxylic acids) per chain.<sup>2</sup> Precisely chain end functionalized linear oligoethylenes are accessible by “chain shuttling” processes.<sup>3,4</sup> As in the Ziegler Alfol process, functionalization occurs in a second step from main-group-metal or zinc alkyls in a stoichiometric fashion. Chain growth occurs catalytically on a smaller amount of transition-metal catalyst.

All of these reported procedures afford linear waxlike oligoethylenes. Highly branched oligoethylenes would also be of interest as functional additives: for example, in lubricants or surface modifiers. Considering possible approaches for their synthesis, the known capability of late-transition-metal catalysts to produce highly branched high-molecular-weight polyethylenes appears attractive. Cationic Pd- and Ni- $\alpha$ -diimine catalysts can undergo extensive “chain walking” during

polymerization.<sup>5</sup> Thus, particularly with the Pd catalysts ethylene is polymerized to a highly branched, high-molecular-weight, entirely amorphous rubbery material. These even contain branches on branches, that is, a hyperbranched<sup>6</sup> structure (also cf. Figure 2 and Scheme 2, left).<sup>5,7,8</sup> In these catalysts, bulky substituents on the diimine ligand are responsible for the formation of high-molecular-weight polymer.<sup>9</sup> Shielding of the apical positions of the square-planar metal centers suppresses chain transfer. At the same time, these bulky substituents also enhance chain growth rates. This has been ascribed to a destabilization of the ground state of the resting state.<sup>5,10</sup> Consequently, less bulky substituted Pd diimine catalysts produce lower molecular weight branched oligomers with low activities.<sup>11</sup>

In addition to the low activity being a limitation of these Pd(II) oligomerization catalysts, catalysts based on nickel are often more favorable in terms of abundant availability of the metal. This is illustrated by the Shell higher olefin process. Here, neutral Ni(II) catalysts convert ethylene to strictly linear longer  $\alpha$ -olefins.<sup>12</sup> Cationic Ni(II) diimine catalysts lacking bulky *o*-aryl substituents also oligomerize ethylene to the linear  $\alpha$ -olefins.<sup>13</sup> Thus, for this type of catalyst the synthesis of highly branched material is usually limited to high molecular weights. For the generation of branched oligoethylenes with neutral Ni(II) catalysts,  $\kappa^2N,O$ -salicylaldiminato complexes are promis-

Received: November 28, 2013

Published: January 22, 2014

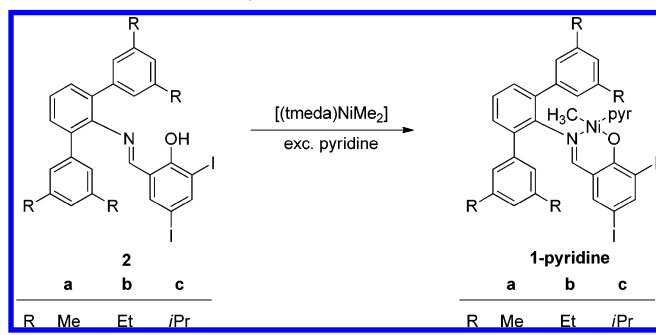
ing candidates. Complexes with the 2,6-diisopropyl *N*-phenyl motif inspired by the aforementioned diimines polymerize ethylene to moderately branched, high-molecular-weight material.<sup>14,15</sup> In *N*-terphenyl-substituted catalysts, substituents (R, cf. Scheme 1) on the peripheral aromatic rings have a remarkable effect on the catalytic properties, despite their remoteness from the active sites.<sup>16</sup> Depending on the substituents, high-molecular-weight linear polyethylene (for R = CF<sub>3</sub>) or low-molecular-weight, highly branched oligomers (for R = CH<sub>3</sub>) are formed.<sup>16</sup> More electron donating substituents favor branch formation and chain transfer, which both occur through  $\beta$ -hydride elimination as the underlying step.<sup>16–18</sup> The observed effect of substituents can be related to very similar barriers of  $\beta$ -hydride elimination ( $\Delta G^\ddagger_{\beta\text{-elim}}$ ) and ethylene insertion chain growth ( $\Delta G^\ddagger_{\text{ins}}$ ).<sup>19</sup> Small relative changes in  $\Delta G^\ddagger_{\beta\text{-elim}}$  and  $\Delta G^\ddagger_{\text{ins}}$  exerted by the electronics of R can then alter the ratio  $\Delta G^\ddagger_{\text{ins}}/\Delta G^\ddagger_{\beta\text{-elim}}$  to a noticeable extent, resulting in entirely different materials obtained.<sup>18b</sup>

In general, there are very few examples of syntheses of ethylene oligomers (<5000 g mol<sup>-1</sup>) with high degrees of branching, and such materials have been little characterized and studied.<sup>20</sup> Functionalized, much less precisely (mono-) functionalized materials have not been reported. We herein give a full account on the efficient synthesis of low-molecular-weight ethylene oligomers with a hyperbranched microstructure and their functionalization to monofunctional compounds.

## RESULTS AND DISCUSSION

**Synthesis of Complexes.** Terphenyl amines with different remote 3',5'-alkyl substituents were prepared by Suzuki coupling of the corresponding 3,5-substituted phenylboronic acid with dibromoaniline. Condensation with 3,5-diiodosalicylaldehyde afforded the salicylaldimines. Reaction with 1.2 equiv of [(tmeda)Ni(CH<sub>3</sub>)<sub>2</sub>] and excess pyridine in benzene at ambient temperature yielded complexes **1a-pyr**, **1b-pyr**, and **1c-pyr** (Scheme 1). Indicative NMR resonances are found at

**Scheme 1. Complexes 1a-pyr, 1b-pyr, and 1c-pyr with Different Remote Alkyl Substituents**



−0.56, −0.54, and −0.54 ppm for the Ni–Me protons for the catalyst precursors **1a-pyr**, **1b-pyr**, and **1c-pyr**, respectively. The presence of only one signal for these groups proves the formation of a single isomer. A single set of resonances is observed for all remote substituents R in **1a-pyr**, **1b-pyr**, and **1c-pyr**, giving no evidence of hindered rotation in the terphenyl moiety in solution on the NMR time scale (for full characterization data cf. the Supporting Information). Single crystals of **1a-pyr** suitable for X-ray diffraction analysis could be obtained within 1 day at −60 °C after layering a solution of the

complex (9 mg) in toluene (0.2 mL) with pentane. The trans coordination geometry of the methyl group and the oxygen donor in Figure 1 agrees with the structures of other

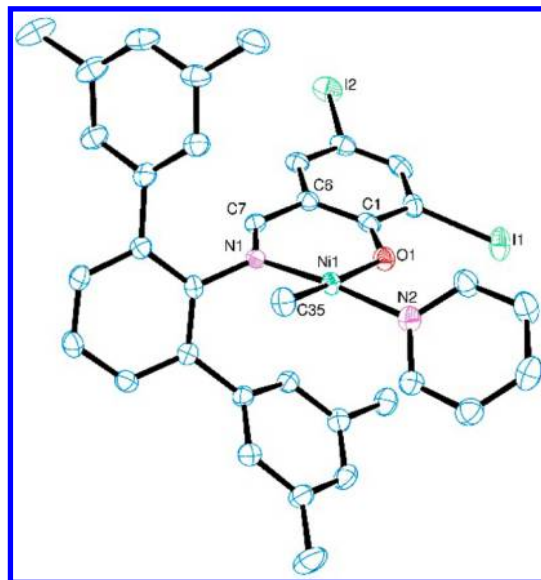


**Figure 1.** X-ray diffraction analysis of the complex **1a-pyr** with 50% probability ellipsoids. Hydrogen atoms are omitted for clarity.

salicylaldimino complexes reported.<sup>14b,16</sup> The deviation of the nickel atom from the root-mean-square plane defined by O1, N1, C35, and N2 amounts to 0.0117(15) Å, which indicates an only minuscule deviation of the coordination geometry of nickel from planarity.

**Catalytic Oligomerization and Microstructure Analysis.** A study of the influence of reaction conditions on the oligomerization with **1a-pyr** (Table 1) reveals that the polymerization temperature has a much more pronounced influence on the molecular weights than the ethylene pressure. As expected, molecular weights increase for low temperatures and high pressures, while the degrees of branching decrease under the same conditions. Molecular weight distributions of  $M_w/M_n \approx 2$  indicate a well-behaved single-site polymerization behavior. Note that GPC analyses are against linear polystyrene standards; thus, they yield apparent molecular weights. As expected, they exceed the true  $M_n$  value from NMR spectroscopy, with a ca. 2-fold deviation. Overall, degrees of branching vary only to a small extent with reaction conditions in the pressure and temperature range studied, from 74 to 81 branches per 1000 C atoms.

However, oligomer yields are strongly dependent on reaction conditions. The highest productivity was observed at intermediate pressures (20–25 bar) and slightly elevated temperatures (40–50 °C). Ethylene mass flow traces reveal that although the activity increases for higher temperatures, significant catalyst degradation occurs, resulting in lower yields (cf. the Supporting Information). For lower temperatures the activity is significantly reduced, but no observable catalyst decomposition occurred over the period of 5 h studied, while at 70 °C the polymerization came to an end after 3 h (Figure S1, Supporting Information).

Microstructure analysis by <sup>13</sup>C NMR revealed the branching patterns of the oligomers produced (Table 2 and Figure 2). Remarkably, they contain hyperbranched structures. This is clearly evidenced by significant amounts of *sec*-butyl groups as

Table 1. Polymerization Results with Complex 1a-pyr under Different Oligomerization Conditions

| entry           | <i>p</i> (bar) | <i>T</i> (°C) | yield (g) | TON <sup>a</sup> | <i>M<sub>n</sub></i> (NMR) <sup>b</sup> | <i>M<sub>n</sub></i> (GPC) <sup>c</sup> | <i>M<sub>w</sub></i> / <i>M<sub>n</sub></i> (GPC) <sup>c</sup> | branches/1000 C <sup>d</sup> |
|-----------------|----------------|---------------|-----------|------------------|---|---|--|------------------------------|
| 1               | 30             | 50            | 54.2      | 48400            | 1300                                    | 2900                                    | 1.7  | 75                           |
| 2               | 25             | 50            | 56.6      | 50500            | 1300                                    | 2600                                    | 1.8  | 75                           |
| 3               | 20             | 50            | 51.3      | 45800            | 1300                                    | 2600                                    | 1.7  | 77                           |
| 4               | 15             | 50            | 45.5      | 40600            | 1200                                    | 2500                                    | 1.7  | 78                           |
| 5               | 10             | 50            | 35.0      | 31300            | 1100                                    | 2500                                    | 1.7  | 78                           |
| 6               | 5              | 50            | 22.6      | 20200            | 1000                                    | 2200                                    | 1.6  | 81                           |
| 7               | 20             | 70            | 12.8      | 11400            | 850                                     | 1800                                    | 1.5  | 80                           |
| 8               | 20             | 60            | 29.6      | 26400            | 1000                                    | 2300                                    | 1.6  | 77                           |
| 9               | 20             | 50            | 51.3      | 45800            | 1300                                    | 2600                                    | 1.7  | 77                           |
| 10              | 20             | 40            | 55.0      | 49100            | 1600                                    | 3500                                    | 1.7  | 77                           |
| 11              | 20             | 30            | 33.1      | 29600            | 2100                                    | 4300                                    | 1.8  | 76                           |
| 12              | 20             | 20            | 13.2      | 11800            | 2600                                    | 5900                                    | 1.7  | 74                           |
| 13 <sup>e</sup> | 20             | 60            | 57.2      | 19300            | 1000                                    | 1600                                    | 2.0  | 77                           |

Reaction conditions (unless stated otherwise): 40 μmol of 1a-pyr in 200 mL of toluene for 5 h. <sup>a</sup>In units of mol of C<sub>2</sub>H<sub>4</sub> (mol of Ni)<sup>-1</sup>. <sup>b</sup>Molecular weights calculated from <sup>1</sup>H NMR intensity ratio of unsaturated end groups vs overall integral. <sup>c</sup>In THF vs polystyrene standards. <sup>d</sup>Degree of branching calculated from <sup>1</sup>H NMR intensity ratio of methyl groups (corrected for saturated end groups) vs overall integral. <sup>e</sup>Reaction conditions: 106 μmol of 1a-pyr in 600 mL of toluene for 5 h. 1a-pyr prepared by in situ catalyst synthesis (cf. the Supporting Information).

Table 2. Microstructure Analysis with Fractional Amounts of Different Branch Lengths<sup>a</sup>

| entry           | <i>p</i> (bar) | <i>T</i> (°C) | branches/1000 C | methyl <sup>a</sup> (%) | ethyl <sup>a</sup> (%) | propyl <sup>a</sup> (%) | C <sub>4+</sub> <sup>a</sup> (%) | sec-butyl <sup>a</sup> (%) |
|-----------------|----------------|---------------|-----------------|-------------------------|------------------------|-------------------------|----------------------------------|----------------------------|
| 1               | 30             | 50            | 75              | 68                      | 12                     | 4                       | 8                                | 7                          |
| 2               | 25             | 50            | 75              | 70                      | 9                      | 5                       | 7                                | 9                          |
| 3               | 20             | 50            | 77              | 70                      | 10                     | 5                       | 8                                | 8                          |
| 4               | 15             | 50            | 78              | 68                      | 11                     | 4                       | 7                                | 11                         |
| 5               | 10             | 50            | 78              | 67                      | 10                     | 3                       | 10                               | 10                         |
| 6               | 5              | 50            | 81              | 63                      | 10                     | 4                       | 9                                | 14                         |
| 7               | 20             | 70            | 80              | 57                      | 14                     | 4                       | 9                                | 15                         |
| 8               | 20             | 60            | 77              | 69                      | 7                      | 4                       | 12                               | 8                          |
| 9               | 20             | 50            | 77              | 70                      | 10                     | 5                       | 8                                | 8                          |
| 10              | 20             | 40            | 77              | 71                      | 8                      | 3                       | 12                               | 6                          |
| 11              | 20             | 30            | 76              | 80                      | 6                      | 3                       | 7                                | 4                          |
| 12              | 20             | 20            | 74              | 81                      | 5                      | 4                       | 6                                | 4                          |
| 13 <sup>b</sup> | 20             | 60            | 77              | 65                      | 9                      | 5                       | 9                                | 9                          |

<sup>a</sup>Percentages of different branch lengths can be calculated from the relative intensity ratios of the methyl (1B<sub>1</sub>, 1B<sub>2</sub>, 1B<sub>3</sub>, B<sub>sec-butyl</sub>) or methine (\*B<sub>4+</sub>) signals of the respective branches in the <sup>13</sup>C NMR spectra. <sup>b</sup>1a-pyr prepared by in situ catalyst synthesis (cf. the Supporting Information).

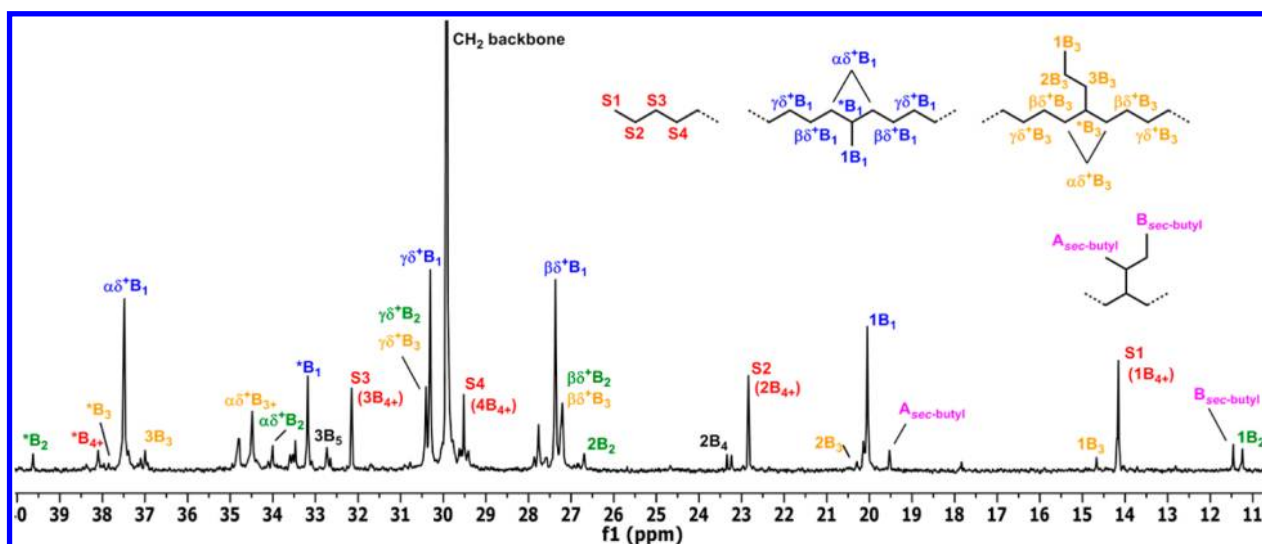


Figure 2. Typical <sup>13</sup>C NMR spectrum of a hyperbranched oligomer. Assignments are numbered according to ref 8,21. Chain ends are assigned with S<sub>1</sub>–S<sub>4</sub>. Branches are labeled as xB<sub>y</sub>, where *y* is the branch length and *x* is the carbon, starting from the methyl end with 1. The methine groups for the different branch lengths are labeled with \*B<sub>y</sub>. A and B are the methyl groups of a sec-butyl branch.

the smallest and detectable branch-on-branch motif. Although the oligomers have similar overall degrees of branching, their microscopic chain architectures differ significantly. While oligomers obtained at low temperatures or high pressures comprise mainly methyl branches and only low amounts of longer chain branches or branch-on-branch structures, those obtained at higher temperatures and low pressures show significantly reduced amounts of these methyl branches in favor of hyperbranched structures, which are found with up to 15% of all branches. As already observed for the molecular weights, the oligomerization temperature also has a more pronounced influence on chain architecture than ethylene pressure. To our knowledge, such hyperbranched microstructures are unprecedented in this low-molecular-weight regime. These low-molecular-weight hyperbranched oligomers are viscous liquids and do not show a melt or crystallization transition during DSC measurements.

A significant simplification of the catalyst precursor could be achieved by eliminating the need for isolated, sensitive [(tmeda)NiMe<sub>2</sub>] used in the preparation of **1a-pyr** to **1c-pyr**. A reaction sequence comprising the reaction of [(tmeda)Ni(OAc)<sub>2</sub>] with methyllithium followed by addition of salicylaldimine **2a** and pyridine and simple evaporation yielded a catalyst which displayed 70% of the activity with regard to isolated **1a-pyr** and yielded an identical oligomer microstructure (cf. entry 13 vs 8 in Tables 1 and 2).

**Dependence of Oligomer Branching Pattern on Catalyst Structure.** The effect of remote alkyl substituents on the catalyst and its potential utility for fine tuning of oligomer microstructures was probed by oligomerizations with **1b-pyr** and **1c-pyr** as catalyst precursors (Tables 3 and 4).

**Table 3. Comparison of Molecular Weights and Branch Distributions for Oligomers Obtained with Catalyst Precursors **1a-pyr**, **1b-pyr**, and **1c-pyr****

| catalyst      | <i>p</i> (bar) | <i>T</i> (°C) | <i>M<sub>n</sub></i> (NMR) <sup>a</sup> | branches/1000 C <sup>b</sup> |
|---------------|----------------|---------------|---|------------------------------|
| <b>1a-pyr</b> | 20             | 60            | 800                                     | 80                           |
| <b>1b-pyr</b> | 20             | 60            | 1500                                    | 73                           |
| <b>1c-pyr</b> | 20             | 60            | 3300                                    | 57                           |
| <b>1a-pyr</b> | 20             | 20            | 2600                                    | 74                           |
| <b>1b-pyr</b> | 20             | 20            | 3700                                    | 65                           |
| <b>1c-pyr</b> | 20             | 20            | 13300                                   | 44                           |

<sup>a</sup>Molecular weights calculated from <sup>1</sup>H NMR intensity ratios of unsaturated end groups vs overall integrals. <sup>b</sup>Degree of branching calculated from <sup>1</sup>H NMR intensity ratios of methyl groups (corrected for saturated end groups) vs overall integrals.

In agreement with the findings that the electronic characteristics of the remote substituents govern the polymerization

behavior, highly branched oligomers are formed with all of these electron-donating substituents. In detail, higher molecular weights and lower degrees of branching are obtained on going from methyl to ethyl and isopropyl substituents. This is in agreement with the finding that sterics have an additional, smaller influence.<sup>18b</sup>

All three catalysts are capable of producing hyperbranched oligomer structures, as indicated by the presence of *sec*-butyl branches (Table 4). Notwithstanding, catalysts **1b-pyr** and **1c-pyr** in particular produce oligomers with distinctively higher percentages of methyl branches (>80%) and minor amounts of longer chain branches. *sec*-Butyl branches, as indicators for a hyperbranched microstructure, can only be obtained at high reaction temperatures using these two catalysts. These findings also show that molecular weights correlate with the overall branch density as well as the average branch length. As a result, higher molecular weight oligomers always come with lower branch densities and almost exclusively comprise methyl branches. Beneficially, desirable features such as high degrees of branching and hyperbranched structures as well as low oligomer molecular weight (ca. 1000) go along with one another.

**Oligomer Functionalization.** Considering that chain termination occurs via β-hydride elimination with the Ni-salicylaldiminato complexes employed, every oligomer chain comprises an unsaturated end group.<sup>22</sup>

Therefore, these oligomers exhibit potential for the synthesis of monofunctional, highly branched ethylene oligomers by postpolymerization functionalization. Due to the extensive chain walking of the catalysts the major end groups found for these ethylene oligomers are internal double bonds and only minor amounts of terminal double bonds (Figure 3).

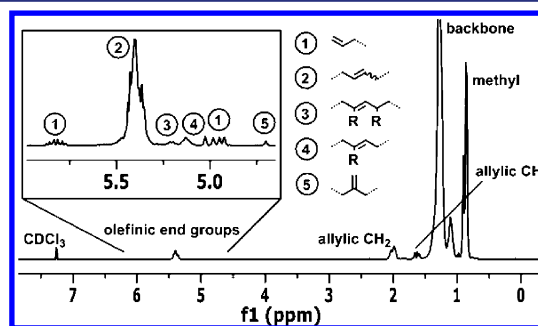


**Figure 3.** Representative <sup>1</sup>H NMR spectrum of unfunctionalized ethylene oligomer.

In terms of a uniform and high reactivity of the products, terminal functional groups are more preferable than a mixture of primary, secondary, and tertiary functional groups. A possible

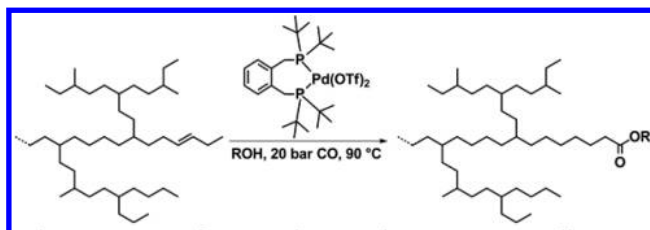
**Table 4. Branching Distribution of Ethylene Oligomers Prepared with Catalyst Precursors **1a-pyr**, **1b-pyr**, and **1c-pyr****

| catalyst      | <i>p</i> (bar) | <i>T</i> (°C) | branches/1000 C <sup>a</sup> | methyl <sup>b</sup> (%) | ethyl <sup>b</sup> (%) | propyl <sup>b</sup> (%) | C <sub>4+</sub> <sup>b</sup> (%) | <i>sec</i> -butyl <sup>b</sup> (%) |
|---------------|----------------|---------------|------------------------------|-------------------------|------------------------|-------------------------|----------------------------------|------------------------------------|
| <b>1a-pyr</b> | 20             | 60            | 80                           | 69                      | 7                      | 4                       | 12                               | 8                                  |
| <b>1b-pyr</b> | 20             | 60            | 73                           | 82                      | 8                      | 3                       | 2                                | 4                                  |
| <b>1c-pyr</b> | 20             | 60            | 57                           | 90                      | 6                      | 1                       | 1                                | 2                                  |
| <b>1a-pyr</b> | 20             | 20            | 74                           | 81                      | 5                      | 4                       | 6                                | 4                                  |
| <b>1b-pyr</b> | 20             | 20            | 65                           | 93                      | 4                      | 1                       | 2                                | 0                                  |
| <b>1c-pyr</b> | 20             | 20            | 44                           | 95                      | 2                      | 2                       | 1                                | 0                                  |

<sup>a</sup>Degree of branching calculated from <sup>1</sup>H NMR intensity ratios of methyl groups vs complete integrals. <sup>b</sup>Percentage of total branches; calculated from intensity ratios of the corresponding signals in <sup>13</sup>C NMR spectra.

approach toward this issue is an isomerization of the internal double bonds to the chain ends. Isomerizing alkoxy-carbonylation allows for converting internal double bonds very selectively to terminal ester groups in a one-step reaction in the presence of carbon monoxide; thus, it appears attractive for the synthesis of end-functionalized oligomers (Scheme 2).<sup>23</sup>

#### Scheme 2. Monofunctionalization by Isomerizing Alkoxy-carbonylation



Typically, the methanol or ethanol coreagent also serves as a solvent. However, this was not suitable for the functionalization of the apolar oligomers due to their lack of solubility. A mixture of pentane and ethanol (1:1) proved to be most suited.

Using  $[(\text{dtbpx})\text{Pd}(\text{OTf})_2]$  ( $\text{dtbpx} = 1,2\text{-bis}[(\text{di-tert-butylphosphino})\text{methyl}]\text{benzene}$ ) as a catalyst precursor,<sup>24</sup> functionalization is evidenced by new signals appearing in the  $^1\text{H}$  NMR spectra at 4.14 and 2.29 ppm (Table 5) using

**Table 5. Conversions in the Isomerizing Alkoxy-carbonylation of Different Oligomers<sup>a</sup>**

| oligomer <sup>b</sup> | $M_n(\text{NMR})$ | branches/1000 C | conversion (%) <sup>c</sup> |
|-----------------------|-------------------|-----------------|-----------------------------|
| 7                     | 850               | 80              | 50                          |
| 6                     | 1000              | 81              | 35                          |
| 1                     | 1300              | 75              | 35                          |
| 12                    | 2600              | 74              | 17                          |

<sup>a</sup>Reaction conditions: 1 g of oligomer, 4 mol % of  $[(\text{dtbpx})\text{Pd}(\text{OTf})_2]$ , 10 mL of pentane/EtOH (1/1), 20 bar of CO, 90 °C, 4 days. <sup>b</sup>Entry number from Table 1. <sup>c</sup>To the primary ethyl ester.

different molecular weight oligomers as starting materials. However, conversion is not complete, as indicated by the observation of residual double bonds. The highest conversion to the ester could be obtained using low-molecular-weight oligomers (850). For higher molecular weights the degrees of functionalization are significantly lower.

However, the reaction is very selective and the primary ester is formed exclusively. No secondary esters are formed, as evidenced by 2D NMR spectroscopy (cf. the Supporting Information). Residual internal and trisubstituted double bonds are found after the reaction, while the terminal vinyl groups are fully converted. Notably, trisubstituted double bonds at a branching point are enriched during the reaction due to the high extent of isomerization (Figure 4). They appear poorly reactive for further conversion and thus represent a limiting factor for the degree of functionalization. Additionally, the lower conversions for higher molecular weights indicate solubility problems of the oligomers in the solvent mixture used.<sup>25</sup>

A second alkoxy-carbonylation of the partially functionalized products resulted in further conversion of internal double bonds with conversions similar to those for the first step, while the amount of the trisubstituted double bonds remains unaltered. This suggests a slow conversion of these double

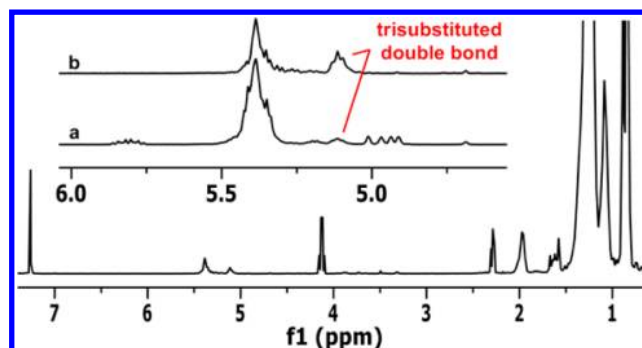


**Figure 4.** Proton NMR spectrum of ester-functionalized oligomer, with the olefinic region before (a) and after functionalization (b) highlighted.

bonds to occur, since a complete lack of reactivity should rather be expected to result in a further enrichment by isomerization. In summary, isomerizing alkoxy-carbonylation allows for a selective terminal postfunctionalization of highly branched oligomers, though quantitative conversion could not be achieved.

An alternative approach to ester-functionalized oligomers is cross metathesis<sup>26,27</sup> of the double bonds with functionalized olefins such as acrylates and subsequent hydrogenation of the double bond. This is a promising reaction also in terms of large-scale synthesis, considering the low catalyst loadings required. However, due to the high amount of internal double bonds present in the oligomers, the reduction of molecular weights is a possible complication.

Cross metathesis of an ethylene oligomer (molecular weight 1600, 78 branches/1000 C atoms) was studied with 10 equiv of ethyl acrylate in the presence of 0.1 mol % of Hoveyda-Grubbs II catalyst (Scheme 3). Quantitative conversion occurred after 4 h at 80 °C, as evidenced by key resonances at 6.97, 5.81, 4.18, and 2.19 ppm in the  $^1\text{H}$  NMR spectrum and the absence of any olefinic resonances of the starting material (cf. the Supporting Information). Identical results in terms of complete functionalization were observed for various other oligomers, independent of their molecular weights and branching densities. The synthesis was readily scalable and was conducted in 50 g batches. From these experiments, no limitation for further scaleup is evident, such as a necessity of excessive solvent volumes or complicated workup procedures.  $^1\text{H}$  NMR spectra and GPC measurements of the oligomers before and after metathesis reveal that molecular weights did not decrease, indicating that the internal double bonds are located close to a chain end. Correspondingly, small  $\alpha,\beta$ -unsaturated ester fragments should be expected as additional metathesis products. To further illuminate this issue, all volatiles were removed after the metathesis reaction under vacuum and collected by condensation at  $-196$  °C. GC-MS analysis showed, aside from the self-metathesis product diethyl fumarate, the formation of the expected fragments from ethyl but-2-enoate to ethyl oct-2-enoate, with the latter being the longest fragment observed (Figure 5). These findings show that, despite the distinct tendency of the catalyst for chain walking, the major amount of internal double bonds is still located near the chain end and is not isomerized deep into the oligomer chain.

Hydrogenation of the double bonds was readily achieved with an ethyl vinyl ether quenched<sup>29</sup> Grubbs I catalyst in quantitative yield at 40 bar of  $\text{H}_2$  and 75 °C after 24 h (Scheme

## Scheme 3. Monofunctionalization with an Ester or Hydroxyl Group, Respectively, via Cross Metathesis

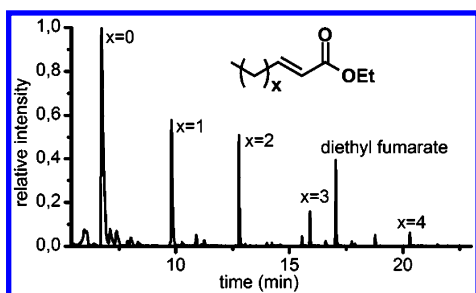
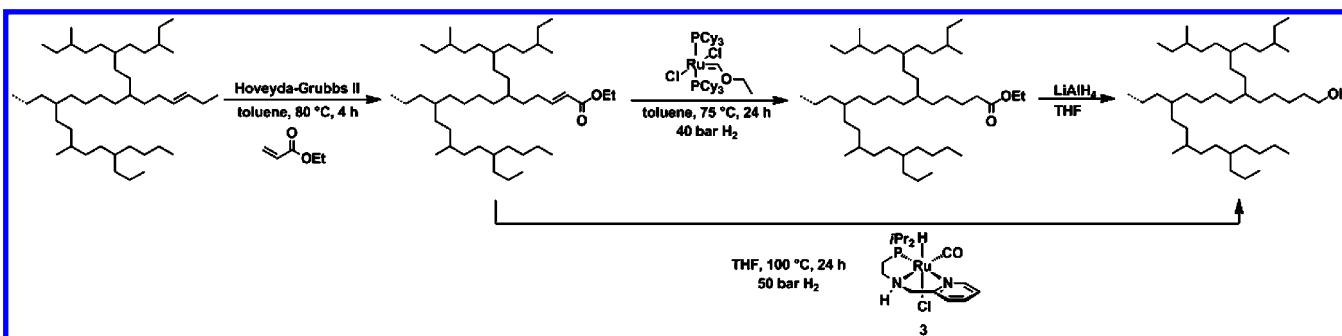


Figure 5. GC trace from GC-MS analysis of the volatile fragments after cross metathesis.<sup>28</sup>

3). Metathesis and hydrogenation of the oligomers could also be performed conveniently in a one-pot reaction. An oligomer (molecular weight 1000, 78 branches/1000 C) was subjected to cross metathesis with ethyl acrylate in a stirred pressure reactor at 80 °C. After 4 h the reaction was quenched with ethyl vinyl ether and pressurized to 40 bar with H<sub>2</sub> for 1 day. The saturated primary carboxylic acid ester product is formed as the only product, as evidenced by proton NMR spectroscopy (Figure 6,

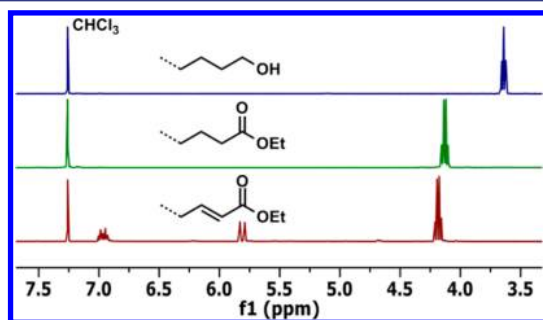


Figure 6. <sup>1</sup>H NMR spectra of the unsaturated ester (bottom), the saturated ester (center), and the hydroxyl-functionalized oligomer (top).

center). An incomplete metathesis functionalization step would result in an apparent increase of molecular weight, as determined from NMR after hydrogenation (cf. the Supporting Information). A found molecular weight of  $M_n$ (NMR) of 950 is further evidence of complete metathesis.

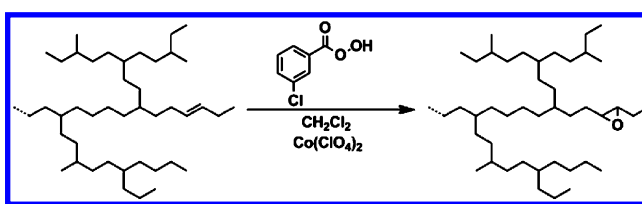
Further functionalization of the ester-substituted apolar branched oligomers was exemplified by conversion to the alcohol. Reduction with LiAlH<sub>4</sub> quantitatively yielded the corresponding hydroxyl-terminated oligomers (Figure 6, top).

However, for a large-scale synthesis the utilization of LiAlH<sub>4</sub> would be prohibitive due to its cost and the tedious workup required for the removal of inorganic salts. The ruthenium

catalyst 3 (Scheme 3), reported by Gusev et al. to convert  $\alpha,\beta$ -unsaturated esters into the saturated alcohols, was found to be suited for the hydrogenation of our ester-functionalized oligomers.<sup>30</sup> The hydroxyl-functionalized oligomers could be obtained quantitatively in a one-step hydrogenation of the unsaturated ester products of the cross-metathesis reaction after 1 day at 50 bar of H<sub>2</sub>, as evidenced by NMR spectroscopy.

In terms of further conversion or application of the highly branched oligomers, for example as macromonomers, reactive epoxide functional groups are also of strong interest. They can be reacted with a range of different nucleophiles, giving access to various different functionalities. Furthermore, epoxidation of double bonds is well documented and has already been applied to polymers. In contrast to the aforementioned functionalization reactions with terminal functional groups, epoxidation mainly yields disubstituted (“internal”) epoxides corresponding to the distribution of double bonds present in the oligomers.

Cobalt-catalyzed epoxidation<sup>31,32</sup> with *m*CPBA or peracetic acid, respectively, was studied (Scheme 4). After 60 min at

Scheme 4. Cobalt-Catalyzed Epoxy Functionalization with *m*CPBA

room temperature virtually complete epoxidation of the internal as well as terminal double bonds was achieved, corresponding to degrees of functionalization of >95%. Key <sup>1</sup>H NMR resonances from the epoxide products arise at 3.1 to 2.5 ppm, while only small amounts (<5%) of terminal double bonds remain unreacted (Figure S14, Supporting Information). Epoxide formation is also evidenced by a new resonance for the C–O stretching of the epoxide at 894.9 cm<sup>-1</sup> in the IR spectrum. The reaction yielded a mixture of internal and terminal epoxides, reflecting the distribution of the double bonds generated in the branching ethylene oligomerization.

Epoxidation of the oligomers proved to be very robust and easily scalable. Functionalization could be performed on the branched oligoethylenes as obtained from oligomerization without further workup (involving e.g. removal of residual catalyst or its deactivation products) on a 50 g scale or larger.

## SUMMARY AND CONCLUSION

Low-molecular-weight products with a hyperbranched microstructure are accessible by oligomerization of ethylene with Ni(II)–salicylaldiminato catalysts. A key to this efficient formation of highly branched oligomers is an *N*-terphenyl motif with remote alkyl substituents. The oligomerization to hyperbranched products proceeds with high rates under moderate conditions of pressure and temperature ( $\leq 20$  atm,  $50$  °C). An in situ prepared catalyst eliminates the necessity of tedious preparation of isolated Ni–dimethyl precursors and thereby resolves an essential limitation of this chemistry. Functionalization of the unsaturated end group of the oligomer chains via cross metathesis or epoxidation, respectively, gives access to monofunctional highly branched ethylene oligomers in essentially quantitative yield. Notably, also in cross metathesis molecular weights are essentially retained and very little material is lost. Overall, all reactions involved are straightforward and readily scalable, as demonstrated by the preparation of 50 g batches. Due to their high reactivity, the primary carboxy or alcohol or disubstituted epoxide groups generated lend themselves to further functionalization. To our knowledge, this is the first report of such hyperbranched monofunctional materials.

## ASSOCIATED CONTENT

### Supporting Information

Text, tables, figures, and CIF files giving complete experimental procedures and analytical data, molecular weight and branching degree calculations, and crystallographic data/processing parameters. This material is available free of charge via the Internet at <http://pubs.acs.org>.

## AUTHOR INFORMATION

### Corresponding Author

stefan.mecking@uni-konstanz.de

### Notes

The authors declare no competing financial interest.

## ACKNOWLEDGMENTS

We thank Jürgen Omeis, Michael Bessel, and Dominika Bernert for fruitful discussions. Financial support by Byk is gratefully acknowledged.

## REFERENCES

- (1) Behr, A.; Ziegler processes. In *Ullmann's Encyclopedia of Industrial Chemistry*; Wiley-VCH: Weinheim, Germany, 2000.
- (2) Wolfmeier, U.; Schmidt, H.; Heinrichs, F.-L.; Michalczyk, G.; Payer, W.; Dietsche, W.; Boehlke, K.; Hohner, G.; Wildgruber, J.; Waxes. In *Ullmann's Encyclopedia of Industrial Chemistry*; Wiley-VCH: Weinheim, Germany, 2000.
- (3) Amin, S. B.; Marks, T. J. *Angew. Chem., Int. Ed.* **2008**, *47*, 2006.
- (4) (a) Britovsek, G. J. P.; Cohen, S. A.; Gibson, V. C.; Maddox, P. J.; van Meurs, M. *Angew. Chem., Int. Ed.* **2002**, *41*, 489. (b) Arriola, D. J.; Carnahan, E. M.; Hustad, P. D.; Kuhlman, R. L.; Wenzel, T. T. *Science* **2006**, *312*, 714. (c) Mazzolini, J.; Espinosa, E.; D'Agosto, F.; Boisson, C. *Polym. Chem.* **2010**, *1*, 793. (d) Gibson, V. C. *Science* **2006**, *312*, 703.
- (5) (a) Johnson, L. K.; Killian, C. M.; Brookhart, M. *J. Am. Chem. Soc.* **1995**, *117*, 6414. (b) Rose, J. M.; Cherian, A. E.; Coates, G. W. *J. Am. Chem. Soc.* **2006**, *128*, 4186.
- (6) (a) *Hyperbranched Polymers* Eds. Yan, D.; Gao, C.; Frey, H. Wiley: Hoboken, 2011. (b) Voit, B. I.; Lederer, A. *Chem. Rev.* **2009**, *109*, 5924–5973. (c) Calderon, M.; Quadir, M. A.; Sharma, S. K.; Haag, R. *Adv. Mater.* **2010**, *22*, 190–218.

- (7) Guan, Z.; Cotts, P. M.; McCord, E. F.; McLain, S. J. *Science* **1999**, *283*, 2059.
- (8) Cotts, P. M.; Guan, Z.; McCord, E.; McLain, S. *Macromolecules* **2000**, *33*, 6945.
- (9) Gates, D. P.; Svejda, S. A.; Oñate, E.; Killian, C. M.; Johnson, L. K.; White, P. S.; Brookhart, M. *Macromolecules* **2000**, *33*, 2320.
- (10) Deng, L.; Woo, T. K.; Cavallo, L.; Margl, P. M.; Ziegler, T. *J. Am. Chem. Soc.* **1997**, *119*, 6177.
- (11) Xiang, P.; Ye, Z.; Subramanian, R. *Polymer* **2011**, *52*, 5027.
- (12) (a) Keim, W. *Chem. Ing. Tech.* **1984**, *56*, 850. (b) Pietsch, J.; Braunstein, P.; Chauvin, Y. *New J. Chem.* **1998**, *22*, 467. (c) Vogt, D.: Organic-organic biphasic catalysis. In *Multiphase Homogeneous Catalysis*; Cornils, B., Herrmann, W. A., Horvath, I. T., Leitner, W., Mecking, S., Olivier-Bourbigou, H., Vogt, D., Eds.; Wiley-VCH: Weinheim, Germany, 2005; pp 330–335. (d) Keim, W. *Angew. Chem. Int. Ed.* **2013**, *52*, 12492.
- (13) (a) Killian, C. M.; Johnson, L. K.; Brookhart, M. *Organometallics* **1997**, *16*, 2005. (b) Svejda, S. A.; Brookhart, M. *Organometallics* **1999**, *18*, 65.
- (14) (a) Wang, C.; Friedrich, S.; Younkin, T. R.; Li, R. T.; Grubbs, R. H.; Bansleben, D. A.; Day, M. W. *Organometallics* **1998**, *17*, 3149. (b) Younkin, T. R.; Connor, E. F.; Henderson, J. I.; Friedrich, S. K.; Grubbs, R. H.; Bansleben, D. A. *Science* **2000**, *287*, 460. (c) Johnson, L. K.; Bennett, A. M. A.; Ittel, S. D.; Wang, L.; Parthasarathy, A.; Hauptman, E.; Simpson, R. D.; Feldman, J.; Coughlin, E. B. (DuPont) WO98/30609, 1998.
- (15) (a) Song, D.-P.; Wang, Y.-X.; Mu, H.-L.; Li, B.-X.; Li, Y.-S. *Organometallics* **2011**, *30*, 925–934. (b) Radlauer, M. R.; Buckley, A. K.; Henling, L. M.; Agapie, T. *J. Am. Chem. Soc.* **2013**, *135*, 3784–3787.
- (16) Zuideveld, M. A.; Wehrmann, P.; Röhr, C.; Mecking, S. *Angew. Chem., Int. Ed.* **2004**, *43*, 869.
- (17) Osichow, A.; Rabe, C.; Vogtt, K.; Narayanan, T.; Harnau, L.; Drechsler, M.; Ballauff, M.; Mecking, S. *J. Am. Chem. Soc.* **2013**, *135*, 11645.
- (18) (a) Göttker-Schnetmann, I.; Wehrmann, P.; Röhr, C.; Mecking, S. *Organometallics* **2007**, *26*, 2348. (b) Bastero, A.; Göttker-Schnetmann, I.; Röhr, C.; Mecking, S. *Adv. Synth. Catal.* **2007**, *349*, 2307. (c) Weberski, M. P.; Chen, C.; Delferro, M.; Zuccaccia, C.; Macchioni, A.; Marks, T. J. *Organometallics* **2012**, *31*, 3773–3789. (d) Osichow, A.; Göttker-Schnetmann, I.; Mecking, S. *Organometallics* **2013**, *32*, 5239–5242. (e) Soshnikov, I. E.; Semikolenova, N. V.; Zakharov, V. A.; Möller, H. M.; Ölscher, F.; Osichow, A.; Göttker-Schnetmann, I.; Mecking, S.; Talsi, E. P.; Bryliakov, K. P. *Chem. Eur. J.* **2013**, *19*, 11409–11417.
- (19) Jenkins, J. C.; Brookhart, M. *J. Am. Chem. Soc.* **2004**, *126*, 5827.
- (20) (a) Daugulis, O.; Brookhart, M. *Organometallics* **2002**, *21*, 5926. (b) Desjardins, S. Y.; Way, A. A.; Murray, M. C.; Adirim, D.; Baird, M. C. *Organometallics* **1998**, *17*, 2382.
- (21) (a) Randall, J. C. *J. Macromol. Sci., Rev. Macromol. Chem. Phys.* **1989**, *C29*, 201. (b) Galland, G. B.; de Souza, R. F.; Mauler, R. S.; Nunes, F. F. *Macromolecules* **1999**, *32*, 1620.
- (22) A possible route of catalyst deactivation involves reductive coupling of a growing Ni–alkyl species with an Ni–H or another Ni–alkyl; cf.: Berkefeld, A.; Mecking, S. *J. Am. Chem. Soc.* **2009**, *131*, 1565–1574. This would result in chains with two saturated end groups. Given that in the oligomerizations studied here ca. 100 oligomer chains are formed per Ni(II) center, any such deactivation reaction would be negligible in terms of oligomer microstructure and analysis.
- (23) (a) Pugh, R. I.; Drent, E.; Pringle, P. G. *Chem. Commun.* **2001**, 1476. (b) Jimenez Rodriguez, C.; Foster, D. F.; Eastham, G. R.; Cole-Hamilton, D. J. *Chem. Commun.* **2004**, 1720.
- (24) Stempfle, F.; Quinzler, D.; Heckler, I.; Mecking, S. *Macromolecules* **2011**, *44*, 4159.
- (25) Decreasing the amount of ethanol resulted in decreased degrees of functionalization. Also, higher dilution or utilization of other solvent mixtures such as pentane/methanol and toluene/ethanol did not enhance conversion.

- (26) Chatterjee, A. K.; Choi, T.-L.; Sanders, D. P.; Grubbs, R. H. *J. Am. Chem. Soc.* **2003**, *125*, 11360.
- (27) Abbas, M.; Slugovc, C. *Monatsh. Chem.* **2012**, *143*, 669.
- (28) Minor peaks not assigned are background originating from the column material.
- (29) (a) Oliván, M.; Caulton, K. G. *Inorg. Chem.* **1999**, *38*, 566. (b) Bielawski, C. W.; Louie, J.; Grubbs, R. H. *J. Am. Chem. Soc.* **2000**, *122*, 12872. (c) Drouin, S. D.; Zamanian, F.; Fogg, D. E. *Organometallics* **2001**, *20*, 5495.
- (30) Spasyuk, D.; Smith, S.; Gusev, D. G. *Angew. Chem., Int. Ed.* **2012**, *51*, 2772.
- (31) Matoishi, K.; Nakai, K.; Nagai, N.; Terao, H.; Fujita, T. *Catal. Today* **2011**, *164*, 2.
- (32) Hyun, M. Y.; Kim, S. H.; Song, Y. J.; Lee, H. G.; Jo, Y. D.; Kim, J. H.; Hwang, I. H.; Noh, J. Y.; Kang, J.; Kim, C. *J. Org. Chem.* **2012**, *77*, 7307.